Journal of Magnetic Resonance **151,** 118–123 (2001)
doi:10.1006/jmre.2001.2348, available online at http://www.idealibrary.com on IDEAL®

In Vivo Detection of the Cyclic Osmoregulated Periplasmic Glucan of *Ralstonia solanacearum* by High-Resolution Magic Angle Spinning NMR

J.-M. Wieruszeski,* A. Bohin,† J.-P. Bohin,† and G. Lippens*,[1]

*CNRS UMR 8525, Institut de Biologie de Lille/Institut Pasteur de Lille, 1 rue du Professeur Calmette, BP447, 59021 Lille Cedex, France; and †CNRS UMR 8576, Université des Sciences et Technologies de Lille, 59655 Villeneuve d'Ascq Cedex, France

Received February 8, 2001; revised April 2, 2001

We investigate the mobility of the osmoregulated periplasmic glucans of *Ralstonia solanacearum* in the bacterial periplasm through the use of high-resolution (HR) NMR spectroscopy under static and magic angle spinning (MAS) conditions. Because the nature of periplasm is far from an isotropic aqueous solution, the molecules could be freely diffusing or rather associated to a periplasmic protein, a membrane protein, a lipid, or the peptidoglycan. HR MAS NMR spectroscopy leads to more reproducible results and allows the *in vivo* detection and characterization of the complex molecule. © 2001 Academic Press

INTRODUCTION

The molecular mechanisms of bacterial virulence are an intense area of research, both from the fundamental and from the applied points of view. The virulence factors displayed by the bacteria, the corresponding host targets, and potential host responses all add to the complex interplay between bacteria and host and can potentially be used to interfere with bacterial infection. Recently, a new genetical approach was developed based on the *Pseudomonas aeruginosa–Caenorhabditis elegans* pathogenesis model (*1*). Analysis of the gene products affected by mutations that attenuated bacterial virulence in a *C. elegans* fast killing model indicated phenazine production as a major molecular toxin. Surprisingly, however, one mutant was impaired in a gene homologous to *hrpM*, previously identified as a locus controlling pathogenecity in the plant pathogen *Pseudomonas syringae* pv. syringae (*2*). The gene product of *hrpM*, or that of its homologue *mdoH* in *Escherichia coli* (*3*), encodes an enzyme involved in the biosynthesis of osmoregulated periplasmic glucans (OPGs). Omnipresent in the periplasmic compartment of Gram-negative bacteria, and with common features in composition (only glucose) and regulation (a higher amount is produced in response to a lower osmolarity of the medium), they do exhibit structural features that are characteristic of a bacterial genus (*4*). How precisely these compounds contribute to bacterial virulence is not known, but at least for the plant pathogen *Erwinia chrysanthemi*, it has been established that, even if the molecules may leave the periplasmic space, they must be present in this cell compartment to play their role(s) in bacterial virulence (*5*).

NMR spectroscopy has been extensively used to establish the primary structure of the OPGs, and recent efforts have attempted to establish their three-dimensional structure. The OPG of *Ralstonia solanacearum*, due to its unique and small size (13 glucose units), its lack of substituents, and the good dispersion of its anomeric proton signals due to a presence of one α-(1-6) linkage that breaks the macroscopic symmetry in the macrocycle (*6, 7*), has been a favorite model in our laboratories (*8*). Despite the accurate measurement of both H_1–H_2' distances over the glyccosidic linkage (*9*) and trans-glycosidic bond coupling constants (*10*), no definite model has come out of these studies, but rather a dynamical model where the macroscopic cycle undergoes large-scale movements on a microsecond time scale has evolved (*11*).

A different question of molecular dynamics, potentially more relevant from the biological point of view, is related to the degree of motional freedom of the OPG molecules in the bacterial periplasm. Their concentration in this cellular compartment can be estimated to be in the range of 10 to 100 mM (*12*). However, since the nature of periplasm is far from isotropic aqueous solution, one can imagine the molecules to be freely diffusing or rather associated to a periplasmic protein, a membrane protein, a lipid, or the peptidoglycan. In this report, we investigate the use of high-resolution NMR spectroscopy, under both static and spinning conditions, to distinguish between those opposite situations. It is found that a major part of the OPG molecules indeed has a significant amount of rotational freedom in the periplasmic space of the bacteria, although it cannot be excluded that a small fraction of immobilized OPG molecules carries the biological function.

MATERIAL AND METHODS

Sample preparation. *R. solanacearum* strain T11 was grown to mid-log phase on a rotary shaker (60 rpm) at 26°C in 50 mL of Luria broth without NaCl. This culture was used to inoculate

[1] To whom correspondence should be addressed.

1090-7807/01 $35.00

600 mL of LOS medium containing 1 g of ^{13}C glucose, 3 g of casein hydrolysate, 2 mg of thiamin, 0.5 mg of $FeSO_4$, 18 mg of $MgCl_2$, 200 mg of $(NH_4)_2SO_4$, and 175 mg of K_2HPO_4 per liter (pH 7.2) and incubated under the same conditions for 24 h (mid-log phase). [U-^{13}C] glucose, and $^{13}C_1$ and $^{13}C_2$ glucose were purchased from Cambridge Isotope Labs (Boston, MA). Cultures were centrifuged at room temperature for 15 min at 7000*g*. Then, the pellets were resuspended in 60 mL of distilled water and centrifuged for 10 min at 3000*g*. Finally, the pellets were resuspended in 3 mL of distilled water (1/200 of the culture volume). This bacterial paste was quickly introduced using a spatula into the NMR rotor or regular 5-mm tube. The purification of the labeled DP13 has been described previously (*6*).

NMR spectroscopy. The NMR experiments were performed on a Bruker DMX-600 spectrometer equipped with a triple-resonance $^1H/^{13}C/^{15}N$ self-shielded *xyz* gradient probehead or a ^1H–^{13}C high-resolution magic angle spinning (HR MAS) NMR probe with uniaxial gradients. All spectra were recorded at a temperature of 28°C. Solution spectra were recorded without sample spinning, whereas the HR MAS spectra were recorded at a 6-kHz spinning rate. Solvent suppression in the 1D spectra was performed with low-power irradiation at the water frequency. Two-dimensional HSQC (heteronuclear single-quantum coherence) and HSQC-TOCSY experiments were performed using standard Bruker pulse programs. Spectra were acquired with 1024×256 complex points and transformed after zero filling to 2048×1024 and multiplication with a $\pi/3$ shifted squared sine in both dimensions. The HSQC-TOCSY spectrum was recorded with a 62-ms MLEV mixing time.

RESULTS AND DISCUSSION

One of the prerequisites of high-resolution NMR is that the external magnetic field is extremely homogeneous over the volume of the detection coil. Modern techniques of magnet and coil design have led to the impressive achievement of a homogeneity smaller than 1 Hz on a total frequency that approaches 1 GHz. When bodies with different magnetic susceptibility are introduced in the sample, this resolution is partially lost due to the macroscopic dipolar fields that are generated at the interfaces of differential magnetic susceptibility. However, as susceptibility differences for entire embryos and aqueous solution were reported to be minimal (*13*), we reasoned that the same might be true for the bacterial cells and therefore first attempted to record spectra on a cell paste in a regular 5-mm NMR tube.

The resulting 1D spectra proved to be very dependent on the sample preparation : although the cellular paste was prepared in a similar way for the four preparations that served as starting material for NMR spectra, the spectra could be qualified as reasonably well resolved to very broad, with intermediate resolution for the other two spectra (Fig. 1). We attribute these quantitative

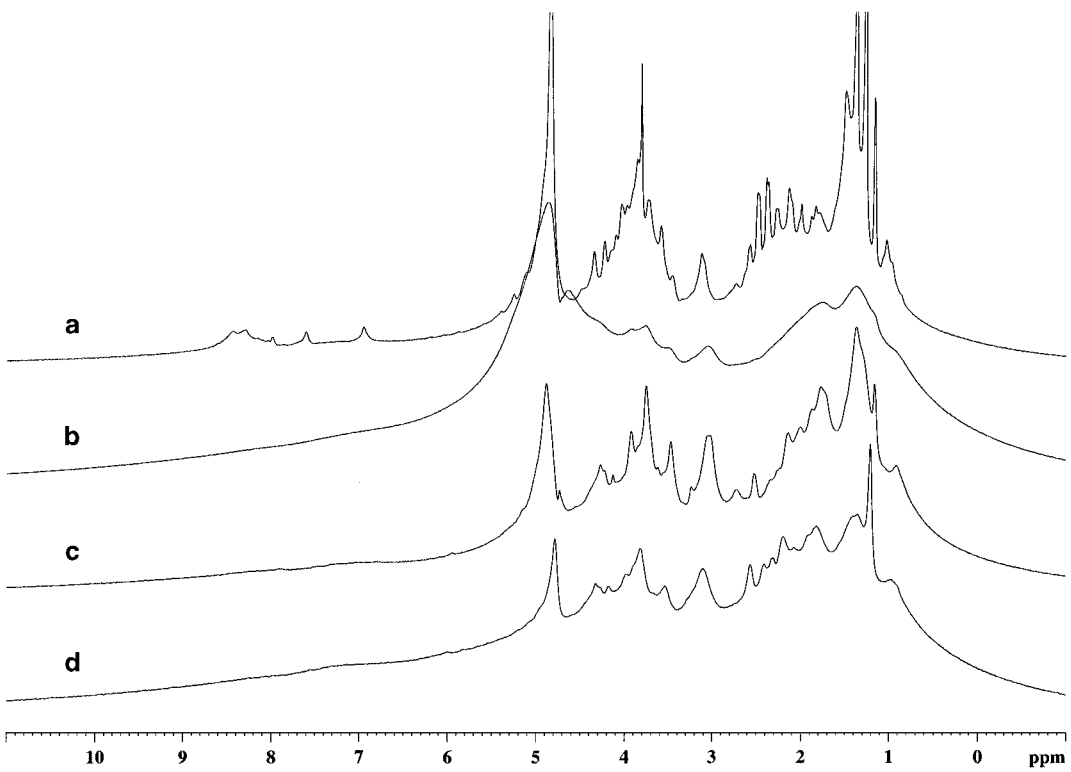

FIG. 1. 1D single pulse spectra of different cell pastes in a regular 5-mm NMR tube. Samples from top to bottom : a cell culture grown on uniformly ^{13}C-labeled glucose (a), grown on $^{13}C_1$-labeled glucose (b, c), and $^{13}C_2$-labeled cell paste (d).

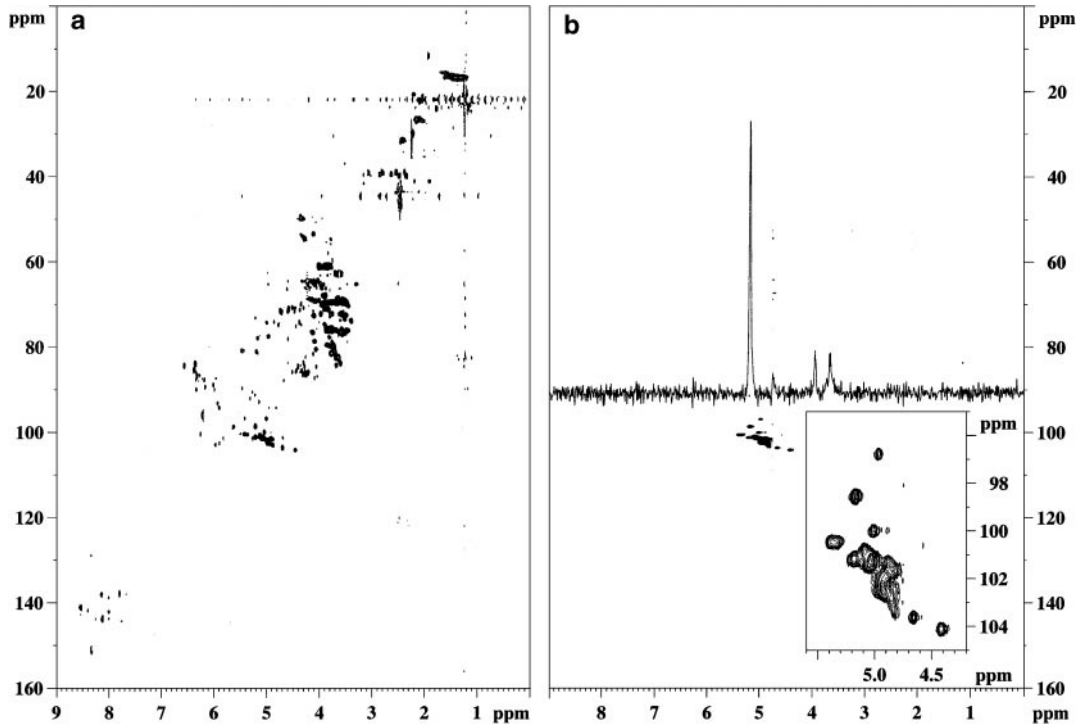

FIG. 2. (a) ^{1}H–^{13}C HSQC spectrum on a cellular paste grown on uniformly ^{13}C-labeled glucose (identical to sample of Fig. 1, top) recorded in a standard 5-mm NMR tube. (b) Same spectrum with the $^{13}C_1$-labeled sample of Fig. 1c. The insert shows an enlargment of the anomeric region. The 1D spectrum corresponds to a trace through the α unit H_1–C_1 correlation (5.18 ppm/98.6 ppm) in the HSQC-TOCSY spectrum of the same sample, connecting the anomeric proton with its H_2 and H_3 protons.

differences in spectral quality mainly to bacterial density gradients in the tube due to initial variations in biomass and to differential sedimentation of the bacteria under the influence of gravity while in the spectrometer. Because both parameters largely escape experimental control, the reproducibility of the experiments was poor. In the best resolved spectrum (Fig. 1, top), we could distinguish some resonances upfield of the residual water line that might correspond to the proton signals of the anomeric protons in the macrocycles.

In order to possibly assign the resonances to the different glucose units, we decided to take profit of the good ^{13}C chemical shift dispersion of the purified molecules (*6*, *7*). Isotopic labeling is straightforward when the bacteria are grown in ^{13}C-labeled glucose, as the OPG molecules are solely constituted of glucose units. The ^{1}H–^{13}C HSQC spectrum on a cellular paste grown on uniformly ^{13}C-labeled glucose confirmed the presence of the anomeric proton–carbon signature of the OPG around 4.9 (^{1}H) and 103 ppm (^{13}C), but many other signals were seen (Fig. 2a). As this dilution of the isotopes into other molecules made the full assignment more hazardous, we decided to grow a new cell culture on $^{13}C_1$-labeled glucose, while simultaneously minimizing the time between the culture and the NMR experiments. A first sample resulted in a very broad proton spectrum (Fig. 1b), and consequently, the HSQC spectrum showed no correlations. With a second preparation, the 1D spectrum was better resolved, even though it remained less resolved than our very first spectrum (Fig. 1c). However, the absence of isotopic dilution made the information in the HSQC spectrum more readily accessible (Fig. 2b). The anomeric region was easily observed, with a distinct cross peak probably corresponding to the unit in the α conformation, the spectral signatures of the alternating β-(1-2) linked units (*8*), and finally the last anomeric proton downfield of the water signal. Whereas this spectral pattern was close to the one observed for the purified molecule (*6*), several additional correlation peaks obscured the identity between the *in vivo* and solution spectrum. While a HSQC-TOCSY spectrum showed the correlations of most anomeric protons with their H2 and H3 protons (Fig. 2b), the absence of similar correlations to protons in the H2/H3 region eliminated some other peaks as potential resonances belonging to the OPG molecule (such as the strong correlation at 5.05 ppm for ^{1}H and 96.5 ppm for ^{13}C). Following centrifugation of the sample after the NMR experiments, we recorded a spectrum on the supernatant. No OPG signals could be detected, indicating that the signals that we observed on the cell containing sample did originate from confined OPG molecules. Finally, we grew the bacteria in a medium supplemented with $^{13}C_2$-labeled glucose. Although the 1D spectrum was of comparable resolution to the one of the $^{13}C_1$-labeled sample (Fig. 1d), the corresponding HSQC spectrum showed some dilution and only weak H2–C_2

correlations. This latter observation is in agreement with the exchange broadening observed for the C_2 carbons of the cyclic molecule in solution (*11*).

Spinning the sample at the magic angle, a technique borrowed from solid-state NMR, has proven an efficient means to average out the macroscopic inhomogeneities in gel-like samples (*14–17*). Known under the name of high-resolution magic angle spinning NMR, it has been successfully applied in the fields of solid phase organic chemistry, peptide synthesis, and polymers (*18–21*). Recently, its clinical use to detect free metabolites in human tissue was described in order to diagnose breast cancer (*22, 23*). An essential limitation of the method is that it only detects molecular species with sufficient mobility to average line broadening partially. The solution NMR results described above indicate that the OPG molecules indeed retain a significant degree of freedom in the periplasm, and HR MAS NMR therefore should be suitable for obtaining an even better resolved spectrum. A new sample of $^{13}C_1$ labeled cells was prepared, and 100 μl of suspension was introduced into a 4-mm rotor. At a spinning rate of 6 kHz, the spectral quality of the 1D spectrum was far superior than anything we had observed in the liquid probe (Fig. 3a), and, more importantly, this spectral quality proved to be very reproducible, as we obtained spectra of similar quality on two additional cell samples. This confirms the possible application for HR MAS NMR to detect and identify intracellularly molecules with a certain mobility and could form the basis for monitoring processes such as drug metabolism or uptake of small molecules, without the need to label the molecules.

When we first acquired a single pulse spectrum without presaturation, two solvent signals could be distinguished. The spectrum of Fig. 3a was acquired with low-power irradiation at the frequency of the main water component, and the residual solvent signal is a result of the large water linewidth in the heterogeneous sample. Alternative to presaturation, solvent suppression based on the differential diffusion properties of the solvent and the molecule of interest has been previously proposed in biomolecular NMR (*24*) and was adapted to HR MAS NMR in order to discriminate between the tethered molecules of interest and the soluble solvent and nonreacted species (*25*). In order to suppress the water signal, we applied to the bacterial suspension the diffusion filter with similar gradient strengths (5 ms of 30 G/cm sinusoidal gradients) and diffusion delays (30 ms) as used for solid phase resins. The OPG resonances were not removed from the spectrum, compatible with their intracellular location, and, surprisingly, a small water component also remained (Fig. 3b). The high diffusion coefficient of liquid water should lead to a complete elimination of all water signal, unless the residual line corresponds to intracellular water that

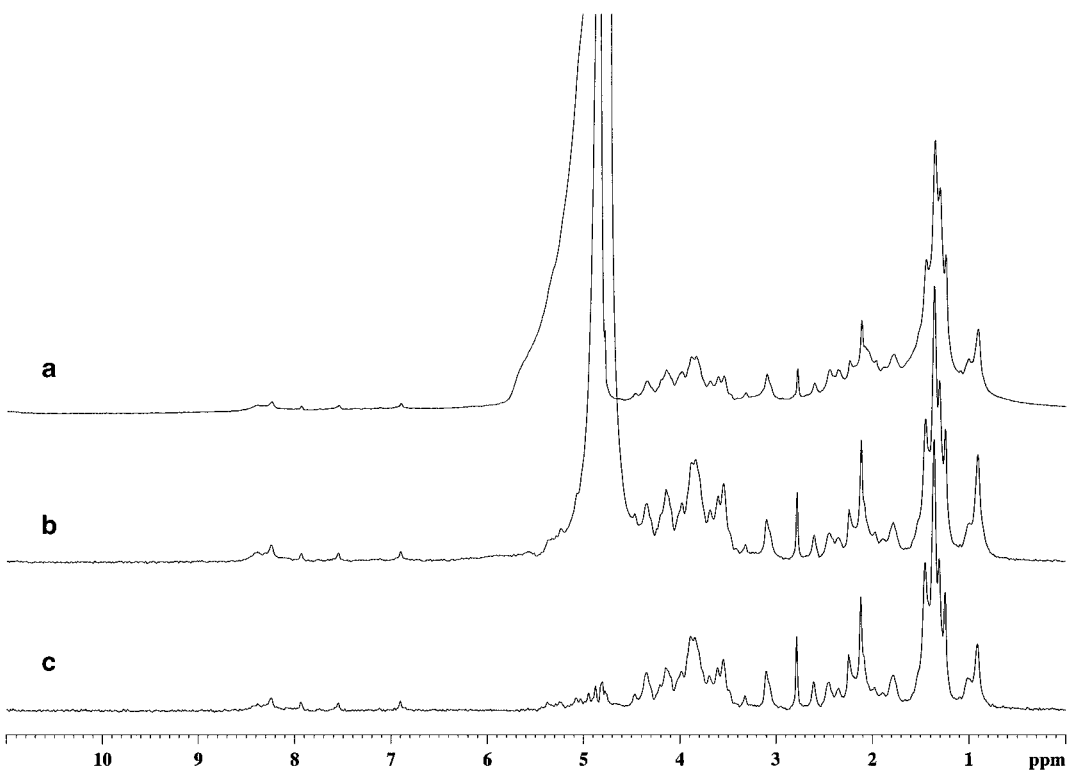

FIG. 3. 1D spectra of different cell pastes in a 4-mm HR MAS rotor spinning at 6 kHz, on a cell culture grown on $^{13}C_1$-labeled glucose. (a) Single pulse experiment with low-power irradiation at the frequency of the main water component for solvent suppression; (b) diffusion filtered 1D spectrum, without further solvent suppression; (c) diffusion filtered 1D spectrum with presaturation at the frequency of the water component seen in spectrum (b).

cannot freely diffuse. When we presaturated this residual watersignal with a weak-power continuous irradiation, the resulting spectrum showed clearly the anomeric proton resonances and the other spectral features characteristic for the OPGs (Fig. 3c).

Although the small inner rotor diameter of 3 mm limits the centrifugal forces, they still might be sufficient to induce bacterial lysis. The OPG molecules could thereby find themselves in a highly viscous environment that would limit their translational diffusion coefficient, allowing their signals to survive in the above-described diffusion experiment. However, not only did we see no evidence for massive bacterial lysis while observing the sample under the microscope after the NMR experiments, but also a control experiment with purified OPG molecules added outside the cells unambiguously proved their intracellular location. We first recorded a regular HSQC and a diffusion-filtered HSQC experiment on the sample grown in $^{13}C_1$-glucose. No significant differences were observed (Figs. 4a and 4b), except for the disappearance of some signals from the diffusion filtered spectrum, corresponding to freely diffusing ^{13}C-labeled molecules. We then recorded the same spectra on a sample grown on unlabeled glucose where the low natural abundance of the ^{13}C isotope yielded an empty spectrum, as expected. To this sample, we added a 2 mM solution of soluble $^{13}C_1$-labeled OPG molecules and recorded again the two HSQC

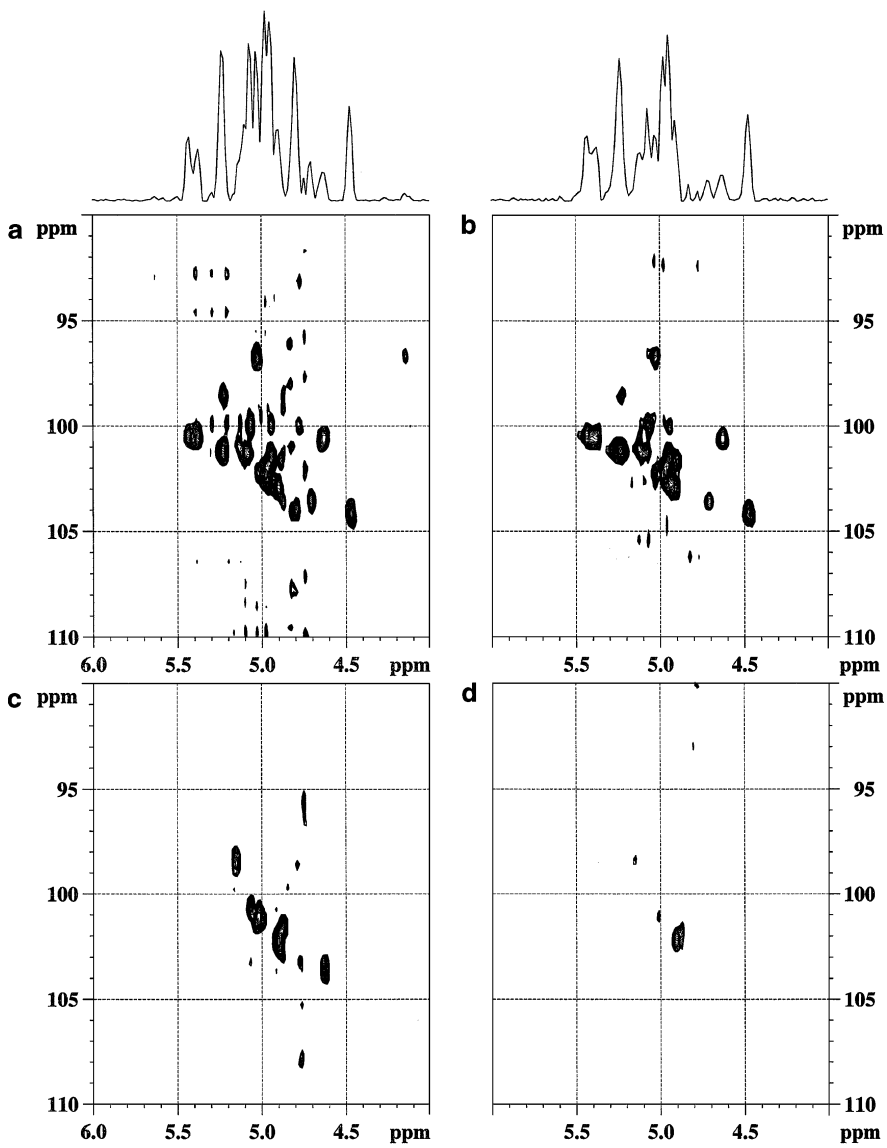

FIG. 4. Regular (left) and diffusion filtered (right) ^1H–^{13}C HSQC spectra of a sample grown on $^{13}C_1$ glucose (top, with proton projection of the zone of interest) or nonlabeled glucose (bottom). To the latter sample, a 2 mM solution of purified $^{13}C_1$-labeled OPGs was added in the rotor. The signals of the OPG molecules in the periplasmic space survive the diffusion filter, whereas the viscosity increase alone is not sufficient to limit the translational diffusion coefficient for the soluble OPG molecules.

spectra. The regular HSQC spectrum confirmed the presence of the OPG molecules (Fig. 4c) and gave signals very close to those of the purified molecules (see below). Translational mobility for the extracellular molecules was, however, large enough to make their signals disappear almost completely in the diffusion filtered experiment (Fig. 4d). This confirms again that the OPG molecules are confined in the periplasmic space of the bacteria.

Already in the solution spectrum on the cell paste grown in $^{13}C_1$ glucose (Fig. 2b), we noted some additional correlation peaks. The presence of additional signals was further confirmed by the HR MAS spectra of the $^{13}C_1$-labeled cells compared to the nonlabeled cells to which we added purified $^{13}C_1$-labeled DP13 molecules (Fig. 4). We had previously observed in our HR MAS studies applied to solid phase organic synthesis that for certain soluble molecules, such as the tetramethylsilane used for reference, two signals appeared in the presence of a polystyrene resin, corresponding to the molecules inside the beads and those in the interstitial solvent (*26*). However, susceptibility gradients here are less severe, and, more important, the spectral changes are expected to be uniform for all signals of a given molecule. Traces through the HSQC-TOCSY spectrum (Fig. 2b) moreover allowed us to conclude that the signals of the glucose units of the OPG are nearly invariant and are all at the same frequency as observed for the purified molecules, leading us to look for other molecular entities that might contribute to the spectrum. Evidently, the Gram-negative *R. solanacearum* bacteria contain a large amount of lipopolysaccharides (LPS), forming the outer leaflet of the outer membrane. These molecules do not diffuse laterally in the membrane plan because the phosphorylated diglucosamines, constitutive of the LPS and present at the interface between lipids and water, strongly interact with each other through cationic interactions. Further out in the chain of the LPS, however, we expect several glucose residues that might have a substantial degree of freedom and thereby contribute to the spectrum. An alternative source of mobile ^{13}C-labeled glucose might be these units integrated into the repetitive unit of the O antigen, but further studies will be necessary to unambiguously assign the additional signals.

CONCLUSION

We have investigated the potential use of NMR to detect a complex biomolecule inside the intact bacterial cell and acquired both homo- and heteronuclear spectra. Spectra required with the traditional hardware for solution spectroscopy were shown to depend heavily on the sample preparation, with parameters such as cell density that are hard to control. Rotating the sample at the magic angle gave very good spectra in a reproducible manner, and pulsed field gradients could be used to prove that the molecules under study are restricted in linear diffusion. For the osmoregulated periplasmic glucans of the phytopathogen *R. solanacearum*, it was shown that a major fraction undergoes significant rotational diffusion in the periplasm, although the functional fraction might be membrane or protein associated.

ACKNOWLEDGMENTS

The 600-MHz facility used in this study was funded by the European Community (FEDER), the Région Nord-Pas de Calais (France), the CNRS, and the Institut Pasteur de Lille. The present study was supported by a grant from the CNRS program "Physics of the Living" accorded to G. Lippens and J.-P. Bohin.

REFERENCES

1. S. Mahajan-Miklos, M.-W. Tan, L. G. Rahme, and F. M. Ausubel, *Cell* **96,** 47 (1999).
2. P. Mukhopadhyay, J. Williams, and D. Mills, *J. Bacteriol.* **170,** 5479 (1988).
3. I. Loubens, L. Debarbieux, A. Bohin, J.-M. Lacroix, and J. P. Bohin, *Mol. Microbiol.* **10,** 329 (1993).
4. J.-P. Bohin, *FEMS Microbiol. Lett.* **186,** 11 (2000).
5. F. Page, S. Altabe, N. Hugouvieux-Cotte-Pattat, J.-M. Lacroix, J. Robert-Baudouy, and J.-P. Bohin, *J. Bacteriol.* **183,** 3134–3141 (2001).
6. P. Talaga, B. Stahl, J.-M. Wieruszeski, F. Hillenkamp, S. Tsuyumu, G. Lippens, and J.-P. Bohin, *J. Bacteriol.* **178,** 2263 (1996).
7. W. S. York, *Carbohydr. Res.* **278**, 205 (1995).
8. G. Lippens and J.-P. Bohin, *in* "NMR in Supramolecular Chemistry," Vol. 191 (M. Pons, Ed.), Nato Advanced Research Series, Kluwer Academic, Dordrecht, 1999.
9. G. Lippens, J.-M. Wieruszeski, P. Talaga, J.-P. Bohin, and H. Desvaux, *J. Am. Chem. Soc.* **118,** 7227–7228 (1996).
10. G. Lippens, J.-M. Wieruszeski, P. Talaga, and J.-P. Bohin, *J. Biomol. NMR* **8,** 311–318 (1996).
11. G. Lippens, J.-M. Wieruszeski, D. Horvath, P. Talaga, and J.-P. Bohin, *J. Am. Chem. Soc.* **120,** 170–177 (1998).
12. D. S. Cayley, H. J. Guttman, and M. T. Record, Jr., *Biophys. J.* **78,** 1748–1764 (2000).
13. J. M. Valles, K. Lin, J. M. Denegre, and K. L. Mowry, *Biophys. J.* **73,** 1130 (1997).
14. W. L. Fitch, G. Detre, C. P. Holmes, J. N. Shoorely, and P. A. Keifer, *J. Org. Chem.* **59,** 7955 (1994).
15. R. C. Anderson, J. P. Stokes, and M. J. Shapiro, *Tetrahedron Lett.* **36,** 5311 (1995).
16. R. C. Anderson, M. A. Jarema, M. J. Shapiro, J. P. Stokes, and M. J. Zilix, *J. Org. Chem.* **60,** 2650 (1995).
17. P. A. Keifer, *J. Org. Chem.* **61,** 1558 (1996).
18. I. Pop, C. Dhalluin, B. Depréz, P. Melnyk, G. Lippens, and A. Tartar, *Tetrahedron* **52,** 12209–12222 (1996).
19. R. Jelinek, A. P. Valente, K. G. Valentine, and S. J. Opella, *J. Magn. Reson.* **125,** 185 (1997).
20. C. Dhalluin, C. Boutillon, A. Tartar, and G. Lippens, *J. Am. Chem. Soc.* **119,** 10494–10500 (1997).
21. G. Lippens, M. Bourdonneau, C. Dhalluin, R. Warrass, T. Richert, C. Seetharaman, C. Boutillon, and M. Piotto, *Current Organic Chemistry* **3,** 147–169 (1999).
22. L. L. Cheng, C. Lean, A. Bogdanova, J. Wright, J. Ackerman, T. Brady, and L. Garrido, *Magn. Reson. Med.* **36,** 653 (1996).
23. L. L. Cheng, I.-W. Chang, B. L. Smith, and R. G. Gonzalez, *J. Magn. Reson.* **135,** 194 (1998).
24. P. C. Van Zijl and C. T. Moonen, *J. Magn. Reson.* **87,** 18 (1990).
25. R. Warrass, J.-M. Wieruszeski, and G. Lippens, *J. Am. Chem. Soc.* **121,** 3787 (1999).
26. R. Warrass and G. Lippens, *in* "Combinatorial Chemistry : Synthesis, Analysis and Screening" (G. Jung, Ed.), Wiley-VCH, 1999.